

**MESOSCOPIC FRACTURES AND AIRPHOTO LINEATIONS  
OF AD-DAWADIMI AREA, PROVINCE OF AR-RIYADH,  
SAUDI ARABIA**

**By**

**Mohammad Ramadan Mohammad**  
Department of Geology, Faculty of  
Science, Alexandria University,  
Alexandria, Egypt.

**ABSTRACT**

Mesoscopic fractures within an area of about 250 sq. km. adjacent to Ad-dawadimi city constitute three systems; J1, J2 and J3 comprising six sets. J1 trends generally NEE and has two sets that are either parallel or including small horizontal dihedral angle. J3 is almost normal to J1 and has two sets with the same conditions. J2 consists of two sets striking diagonally to J1 and J3 and including horizontal dihedral angle, approximate average;  $55^{\circ}$  to  $70^{\circ}$ , in between and around J1. The fractures cut through Precambrian rocks.

Photographic lineations within an area of about 2100 sq.Km. including the previous area are analysed. They show preferred directions to NNE, NE, E and SEE. Such trends are well correlated to J1 and J2 but poorly correlated to J3. Local differences in the preferred directions are related to variable multi-stress directions probably originated from the tensional character of the old magmatism within this part of the Arabian shield.

Fractures in the studied area are related to two episodes. The earlier one developed multidirectional tensional fractures mostly filled by dyke intrusions. The succeeding episode, probably caused by NEE-SWW compression, led to the formation of the six sets of fractures related mostly to J1, J2 and J3.

## INTRODUCTION

The studied area occurs at the extreme eastern parts of the Arabian shield, including the city of Ad-dawadimi at its northern parts (Fig. 1). It is bounded by the longitudes  $44^{\circ} 1'$  &  $44^{\circ} 33' E$ , and the latitudes  $24^{\circ} 19'$  &  $24^{\circ} 30' N$ , comprising about 2100 sq. Km. The air photographic linear features are studied within the whole area, inside dashed line rectangle in Figure 1 - b, while the mesoscopic fractures are studied in the field within a part of the area, mostly rectangle B of Figure 5.

The general geology of the area, after Bramkamp et al (1963), is shown in Figure 1 - b. Gneissic granite covers most of the area, an amphibolite complex forms a block of a boss dimensions and chlorite and sericite schist appears at the eastern and western borders of the studied area. Numerous dykes cut the area.

Two Precambrian orogenic cycles affected the region, named by Brown (1970 & 1971) as Higaz and Najd orogenies. The older one "Higaz" was dominated by east - west compression giving north - northeasterly to meridional structural belts (folds and faults, locally overthrust beds). The succeeding and partially overlapping orogeny "Najd" is distinguished by a change in direction of pressure giving rise to northwest strike - slip faults (Fig. 2).

Stoesser and Camp (1984) divide the Arabian shield into five microplates (terraces) separated by four suture zones. The studied area occurs within the Al Amar suture zone (Fig. 2) that separates the two microplates named Ar Rayn to the east and Affif to the west of it. Collision between them resulted in widespread '670 - 360' Mesozoic plutonism (Clavez and others 1983) with a NNW linear pattern, approximate trend of which is about  $N155^{\circ}$ .

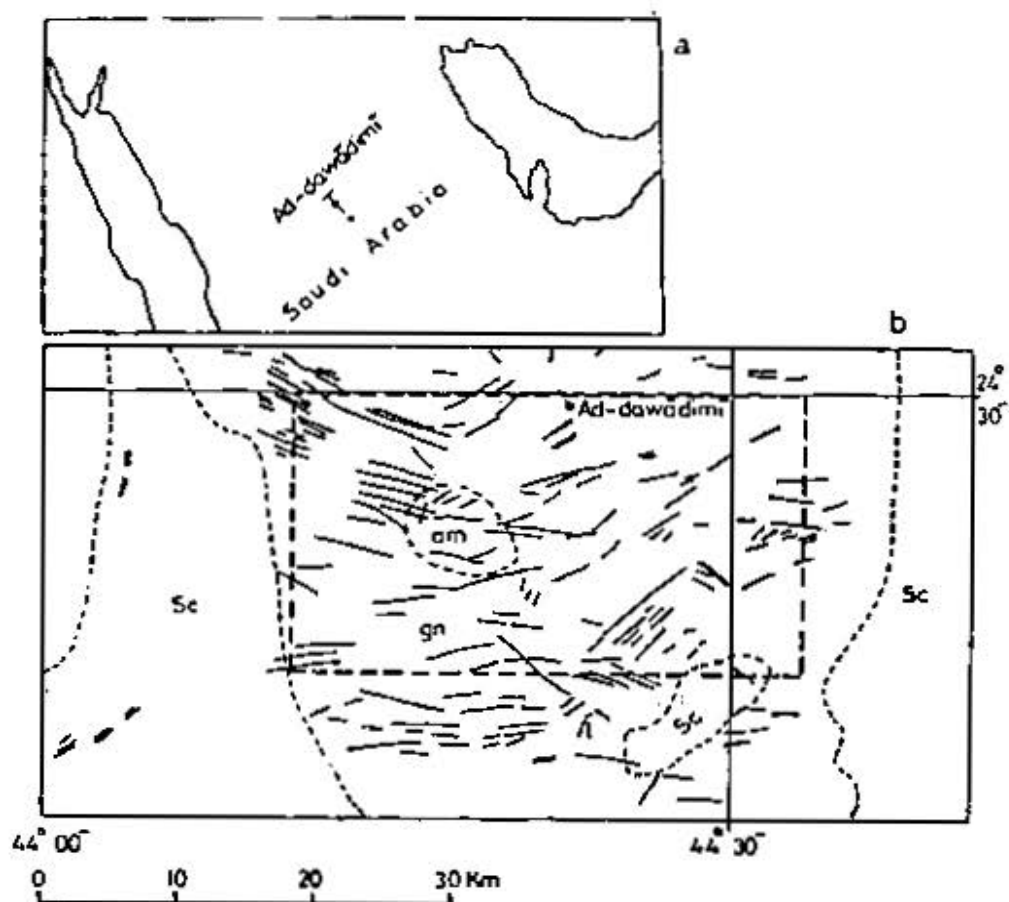


Fig.1-a; Location map of the studied area. b; General geology of the region including the studied area (inside dashed line rectangle); am; amphibolite, gn gneissic granite, sc; schist and —; dykes (after Bramkamp et al 1963)

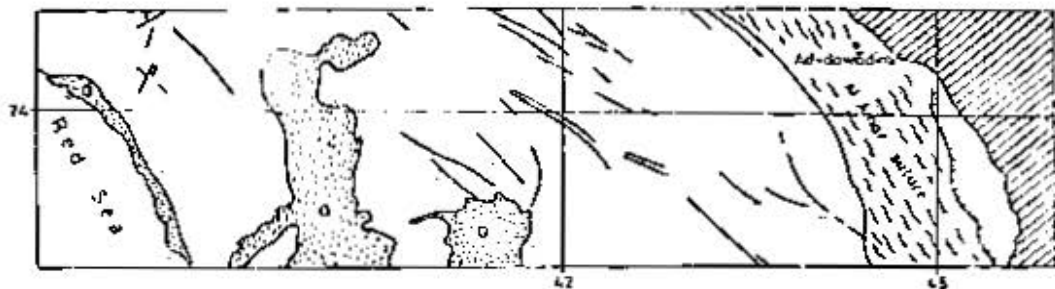


Fig. 2

Fig. 2-Regional fractures, mostly transcurrent faults, cutting the Arabian shield adjacent to the project area: Arabian shield, Arabian shelf and Quaternary (After Brown 1971) Orogenic belt of Al Amar suture within the shield (after Stoesser and Camp 1984)

Fig. 3-A; Mean strikes of the mesofractures measured in the field, amphibolite, granite, B; Pole contour diagram of these fractures 169 poles, > 5.3%, 3% to 5.3% 0.6% to 3% and < 0.6%, C; Mean planes of the maxima shown in B

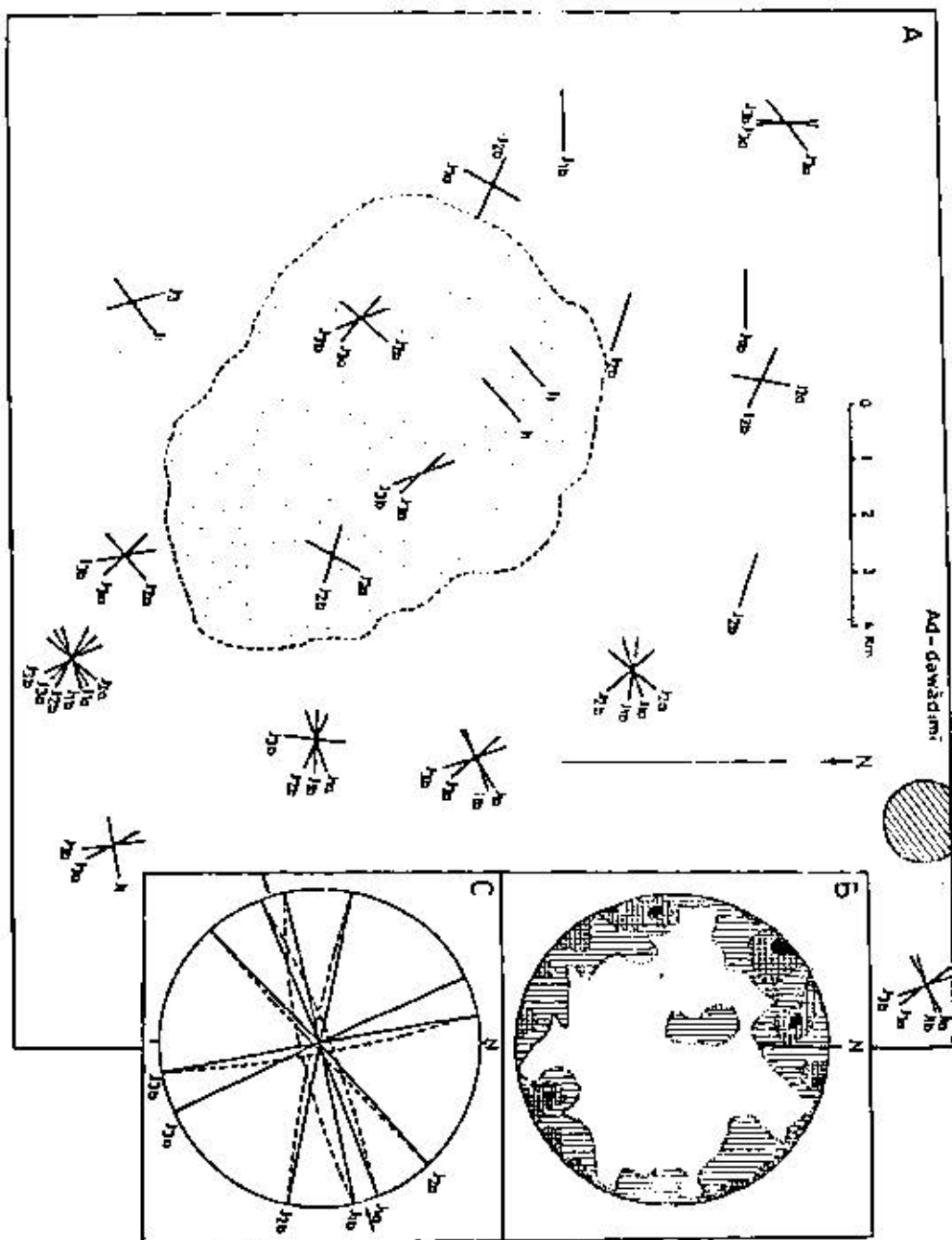


FIG. 3

## MESOSCOPIC FRACTURES

Fracture cleavage, Joints, minor faults and fracture filled by rock and mineral dykes are measured, dip and strike, and noticed in the field at twenty stations (Fig. 3). The stations occur mostly within rectangle B of Figure 5 which is relatively rich by photographic lineations. Fracture cleavage are almost well developed in the dyke intrusions, parallel to the walls of the dykes or slightly inclined (Pl. I - A). They are considered here as defined by Spencer (1977) as closely spaced parallel joints and fractures. The density of them in the studied area reached 90 planes within one meter length normal to fracture planes.

The jointing ranges from small planes cutting for small vertical distances; usually less than 5 meters, and medium size joints, roughly between 5 and 15 meters vertical length to master joints extending for more than 20 meters. The density varies from 50 per 10 meters length normal to the joint planes for smaller joints to 5 or even less for the master joints.

The mesoscopic fractures exist mostly as vertical to subvertical planes. Some fractures were opened and filled by igneous dykes or by hydrothermal minerals (Pl. I - B), such fractures are considered as extension fractures. Those that are straight, tight and usually without filling materials are considered as shear fractures. They exist in the studied area in two sets (J2a and J2b) comprising horizontal acute angle of about  $40^\circ$  to  $80^\circ$  in between, the bisectrix of which trends NEE - SWW (Fig. 3 - C). Fracture cleavage are developed also parallel to them (Pl. I - A).

Six sets of fractures (Fig. 3 - A) are distinguished by field measurements. The poles of the fracture planes projected on the lower hemisphere equal area Schmidt net and contoured by the Schmidt grid method (Fig. 3 - B & - C) show also six maxima comparable to field sets. Azimuthal directions, clockwise from N to E, of the mean fracture planes of each set as detected by both field measurements and pole contour diagram are shown in Table 1, classified under the three systems J1, J2 and J3, each includes two sets; a and b.

Table 1 : Mean planes for the fracture sets  
of the studied area.

System	Set	Trend	
		Field data	Pole maxima
J1	J1 a	N060° E	N069° E
	J1 b	075	078
J2	J2 a	040	047
	J2 b	110	102
J3	J3 a	145	155
	J3 b	165	171

J1 is almost normal to J3 (Fig. 3 - C) and the two sets forming each of them are either parallel or comprising small dihedral horizontal angle in between (Fig. 3). Both are interpreted as extension fractures. Some of these fractures were filled by igneous rocks and minerals, later cut by younger trends of J1, J2 and J3. Younger fractures of J1 and J3 are almost barren, slightly opened and sometimes irregular with matching margins.

In order to distinguish the older extensional trends, an azimuth frequency diagram (Fig. 4 - B) is plotted for the mesoscopic and larger dykes, approximately within the area of field measurements (Fig. 4 - A). This diagram shows that the dykes are mostly diffused within a broad azimuthal area between NE clockwise to SEE including three preferred trends; (N030° - 040°), (N050° - 060°) and (N090° - 110°) which are subparallel to J2 a, J1 and J2 b respectively. They almost reflect directions of old tension fractures with local stress variations. El-Etr (1971) discussed a similar problem. He stated that once a tension set of fractures is filled by dyke intrusions it ceases to act as channel ways for further injections anymore. This leads to local changes of stress orientation allowing the development of new set of tension fractures around different trend. These multidirectional older extension fractures were almost superimposed by younger systematic sets of mesoscopic fractures of the systems J1, J2 and J3.

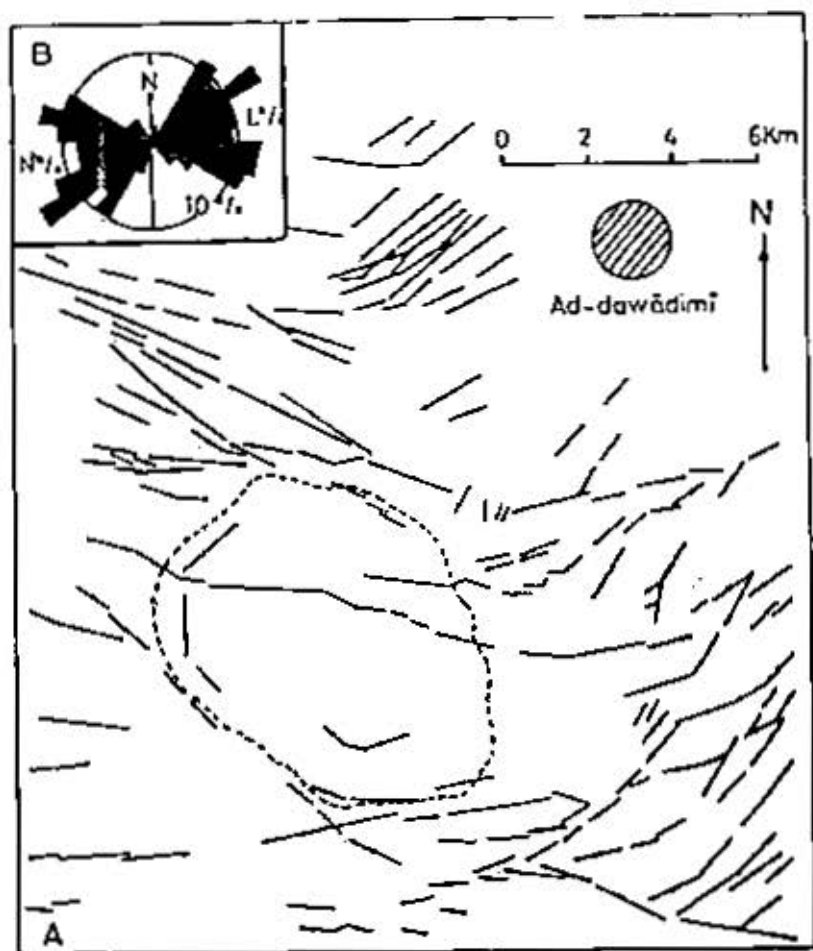


Fig. 4-A; Dyke lineations, nearly for area of rectangle B of Figure 5, B; Azimuth frequency diagram for these lineations

The northwesterly trending normal strike-slip faults (Fig. 2), having approximately the general trend  $N130^\circ$ , do not show good correlation with any of the identified sets of fractures. Better correlation is obtained if considering the NNW linear pattern related to the Al Amar suture zone (Fig. 2) and trending approximately  $N155^\circ$ . This trend may be considered roughly as parallel to the acute bisectrix of the angle between J3 a and J3 b. J1 is generally normal to it. The normal to this trend may be considered as the acute bisectrix between the two conjugate sets J2 a and J2b, the mean of the acute angle in between ranges between  $55^\circ$  and  $70^\circ$ .

A compressional stress trending NNW-SSE (nearly  $N037.5^\circ$ ), as indicated by the two arrows in Figure 3 - C, acting more probably after the granitoid emplacement; contemporaneous and probably also after injection of the dykes, is proposed as responsible for the identified three systems. The model presented by Price (1966, p. 144) supports this view. Such stress is responsible for J1 (tension) parallel to it, J3 (tension) normal to it and for the two shear fracture sets of J2 oblique on both sides of it.

### AIRPHOTO LINEATIONS

Uncontrolled mosaic for the studied area is built by aerial vertical photographs of average scale 1 to 80.000. Linear features of the area are plotted using this mosaic. About one thousand of such features are distinguished (Fig. 5). They include dyke ridges, fractures without injections, linear valleys, scarps, tonal variations, and linears separating geologic features of different textures. The area is almost dry and barren without vegetation lineaments.

In order to obtain a homogeneity in the prepared orientation diagrams, the area is subdivided into 8 rectangles and an azimuth frequency diagram is built for each one (Fig. 6). The eastern halves of the diagrams represent the length percentages of total lineations within azimuthal classes of  $10^\circ$  from the sum lengths of lineations in each rectangle while the western halves represent the corresponding number percentages.

The plotted linear features are almost microlinears; below 2 Km. in length, only about 5% from the total number of linears exceeds 2 Km. and up to 5 Km. in length.

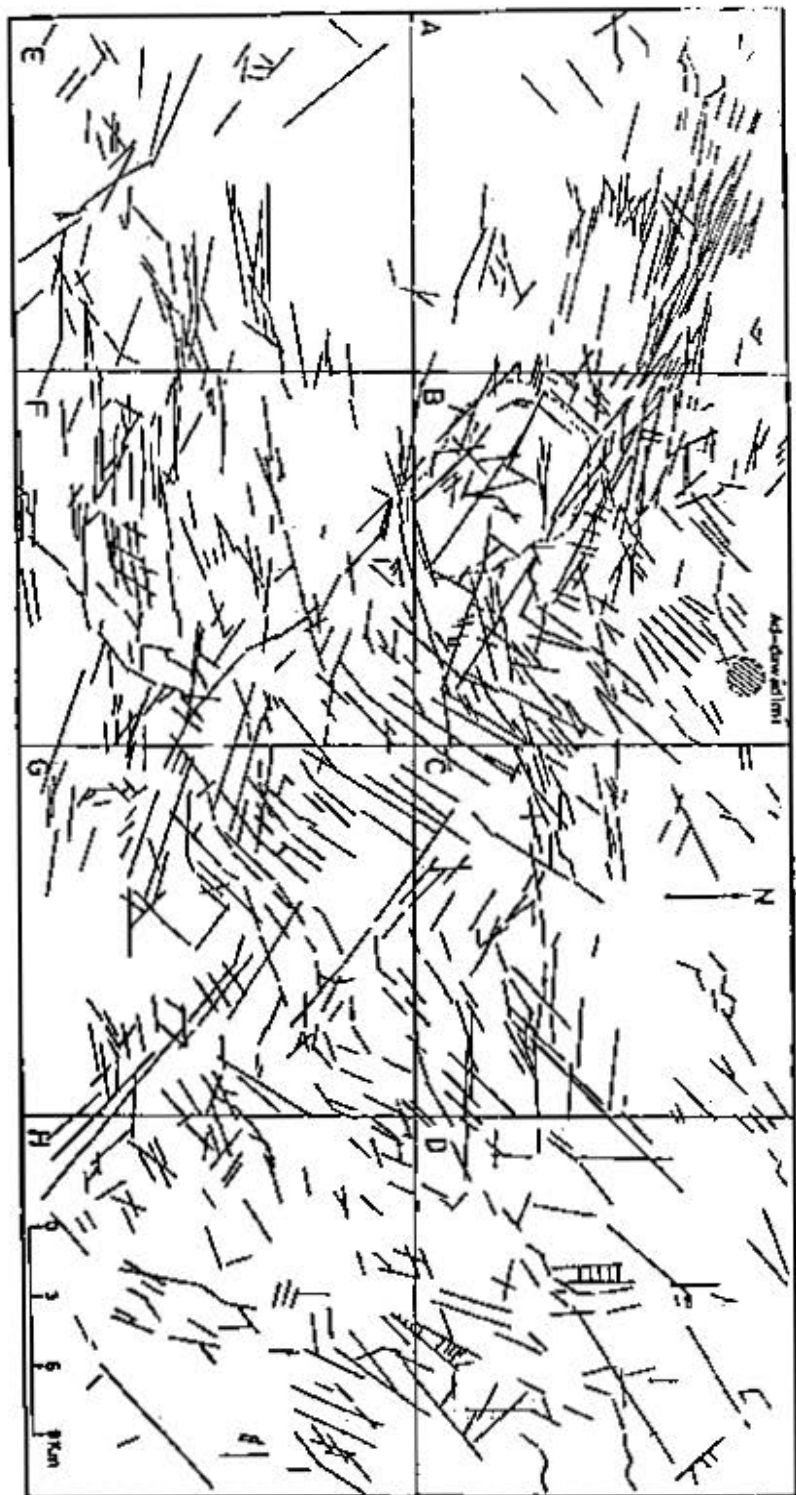


Fig. 5. Air photo lineations of the studied area

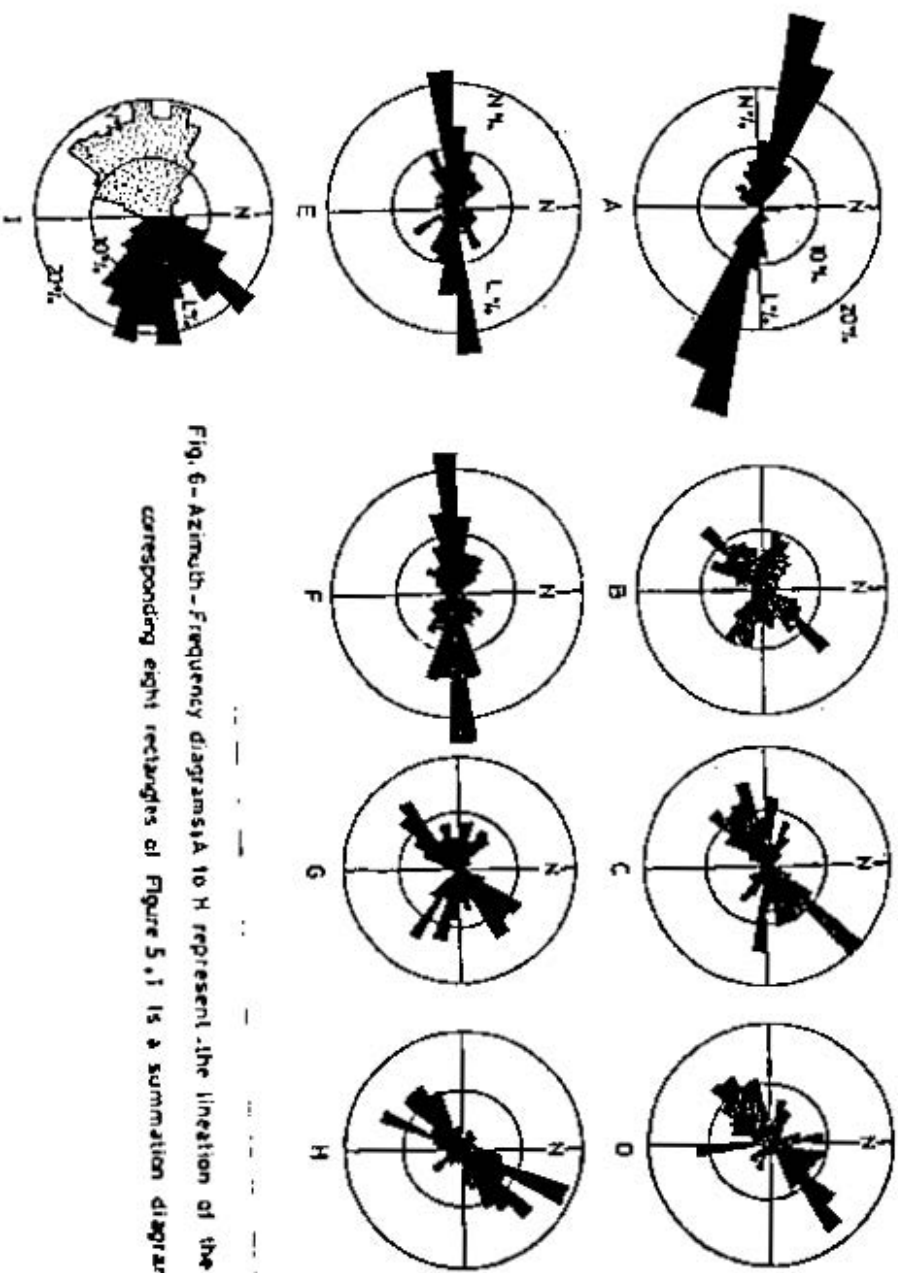


Fig. 6-Azimuth-Frequency diagrams A to H represent the lineation of the corresponding eight rectangles of Figure 5. I is a summation diagram.

Preferred directions appeared on the azimuth frequency diagrams are generally to NNE, NE, E and SEE (Fig. 6) with slight local variations. A preferred trend to north appears only in rectangle D. The length percentages of all the maxima are almost slightly larger than the corresponding number percentages, either both are nearly equal. This may denote that they probably reflect mesoscopic to regional fractures rather than microfractures and joints.

Nearly all the preferred trends have diffused lineations forming smaller maxima around it, sometimes of considerable frequencies as shown in the rectangles A & F, Figure 6. They represent local scattered mesoscopic fractures subparallel to the adjacent preferred trends.

Preferred trends that may be regarded as being represented locally as well as regionally are those in NE; (N030° - 040°) and (N040° - 060°) and SEE; (N100° - 120°) and (N120° - 130°) directions.

The summation diagram (Fig. 6-1) representing all the lineations in the area shows preferred trends in NE; (N040° - 050°), E; (N080° - 090°) and SEE; (N100° - 110°).

## LINEATIONS AND FRACTURES

Comparing the photographic lineations with the fracture sets obtained by field measurements, especially those of rectangle B of Figure 5, in which field measurements were focused, the preferred lineation trends are almost subparallel to the four sets of fractures forming J1 and J2. J3 has no comparable lineation predominant trend. Most of the lineations have probably developed along older trends of J1 and J2; Precambrian multidirectional tensional fractures, while younger trends of them together with J3 are not yet expressed topographically obviously as the older ones.

## REFERENCES

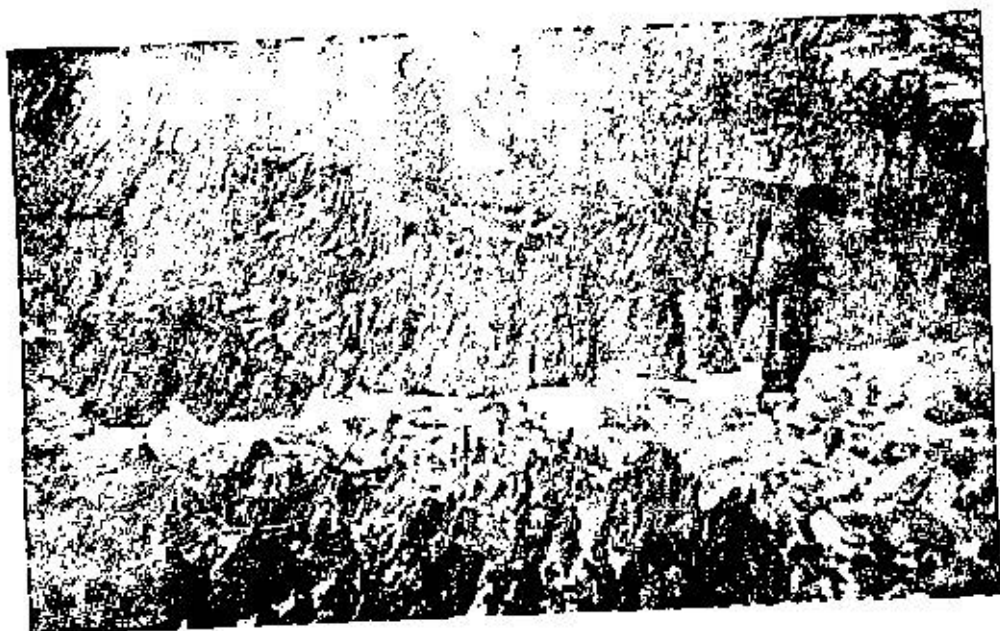
- Bramkamp, R.A., Ramirez, L.F., Brown, G.F. and Pocock, A.E., 1963, Geologic map of the Wadi Ar-Rimah quadrangle, Kingdom of

Saudi Arabia: U.S. Geol. Survey Misc. Geol. Inv. Map  
I 206B, Scale 1:500,000.

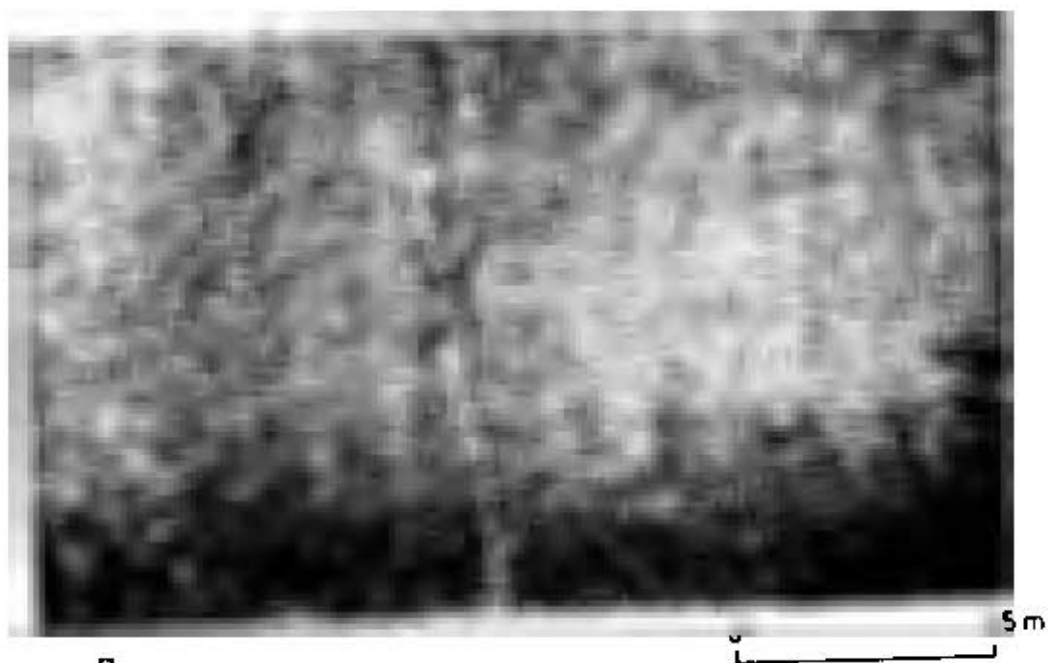
- Brown, G.F., 1970, Eastern margin of the Red Sea and the coastal structures in Saudi Arabia: Royal Soc. (London) Philos. Trans., v. 267, no. 1181, p. 75-89.
- Brown, G.F., 1971, Tectonic map of the Arabian Peninsula: U.S. Geol. Survey Saudi Arabian Project rept. 134.
- Calvez, J.Y., Alsac, C., Delfour, J., Kemp, J., and Pellaton, C., 1983, Geological evolution of western, central, and eastern parts of northern Precambrian shield, Kingdom of Saudi Arabia: Deputy Ministry for Mineral Resources Open-File Report B GM-OF-03-17, p. 57.
- El-Etr, H.A., 1971, Analysis of airphoto lineations of Darheeb district, south Eastern Desert: Annals Geol. Survey, Egypt, v.1, p. 93-108.
- Girdler, R.W. (ed), 1972, East African rifts: Amsterdam, Elsevier.
- McConnell, R.B., 1972, Geological development of the rift system of Eastern Africa: Geol. Soc. America Bull., v.83, no. 9, p. 2549ff.
- Price, N.J., 1966, Fault and joint development in brittle and semi-brittle rock: Oxford, Pergamon.
- Spencer, E.W., 1977, Introduction to the structure of the earth: New York, McGraw-Hill.
- Stoeser, D.B. and Camp, V.E., 1984, Pan-African microplate accretion of the Arabian shield: Saudi Arabian Deputy Ministry for Mineral Resources, Open-File Report USGS-TR-04-17, p.26.

## PLATE I

- A Fracture cleavage cutting through thick basic igneous dyke and existing in two sets, J2a; approximately normal to the plane of the photograph and J2b; slightly oblique on this plane. the hammer rests on a surface of J2b.
  
- B Extension fractures (J3) filled by thin hydrothermal mineral veinlets.



A



B

PLATE I